Molecular Orientation of High-Density Polyethylene Fibers Characterized by Polarized Raman Spectroscopy

Mario J. Citra, D. Bruce Chase,* Richard M. Ikeda, and Kenncorwin H. Gardner

E. I. Du Pont Central Research and Development Experimental Station, Wilmington, Delaware 19880

Received December 8, 1994; Revised Manuscript Received February 27, 1995®

ABSTRACT: Polarized Raman spectroscopic measurements were performed on a uniaxially oriented high-density polyethylene (HDPE) fiber. The second and fourth coefficients of the orientation distribution function, $\langle P_2(\cos\theta)\rangle$ and $\langle P_4(\cos\theta)\rangle$, respectively, have been quantitatively determined from the scattering intensities of the bands at 1130 and 1418 cm^{-1}. This work represents the first quantitative determination of the orientation parameters for a HDPE fiber by Raman spectroscopy. The values of $\langle P_2(\cos\theta)\rangle$ calculated from the Raman experiments are shown to be in excellent agreement with the calculated value obtained by X-ray diffraction.

Introduction

High-density polyethylene (HDPE) is a predominantly crystalline, linear form of polyethylene that is often used to produce films, containers, and high-strength fibers. The physical properties of the resultant materials are dependent on many characteristics such as branching and crystallinity. Orientation of molecular chains can also play a dramatic role in determining the mechanical properties; therefore the study of molecular orientation in polymer films and fibers is of considerable interest.

Several experimental methods have been employed to characterize the orientation of crystalline and semicrystalline polymers. Birefringence, nuclear magnetic resonance, X-ray diffraction, and infrared linear dichroism are among the most popular methods used to characterize different aspects of molecular order. Each of these techniques has inherent advantages and disadvantages when compared with one another.[1]

Polarized Raman spectroscopy can also be used to probe the molecular orientation in polymers.[2-6] The scattering nature of Raman spectroscopy provides an effective means for the study of samples that do not sufficiently transmit radiation, provided care is taken to minimize polarization scrambling by the sample. Linear dichroism and birefringence measurements often cannot be used for thick polymer specimens. A second advantage of Raman spectroscopy is the ability to determine both the second and fourth coefficients of the orientation distribution function. Linear dichroism and birefringence measurements are sensitive only to the second moment of the expansion. Unfortunately, Raman spectroscopy is more complex from both an experimental and theoretical point of view when compared to linear dichroism and birefringence. Not surprisingly, few quantitative Raman spectroscopic measurements of molecular order have appeared in the literature over the past 20 years. The majority of these studies have usually been applied to polymer film samples. We are aware of only two studies that have utilized Raman spectroscopy to calculate the order parameters of fiber samples.[7,8] These studies were conducted on poly(ethylene terephthalate)[7,8] and poly(ethylene naphthalenedicarboxylate) samples.[8] Only three intensity measurements were obtained and the Raman tensors for the vibrational modes studied were approximated as possessing cylindrical symmetry.[7,8] Since the Raman tensor of HDPE is not cylindrical for the majority of vibrational modes,[6] such approximations are inadequate for the present study.

We present the first quantitative study regarding the molecular orientation of HDPE fibers by polarized Raman spectroscopy. Recording spectra with both a right-angle scattering geometry and a backward scattering geometry, all necessary intensities required to calculate the second and fourth coefficients of the orientation distribution function are obtained.

Theory

The explicit theory and procedure for determining the orientation of polymer samples by Raman spectroscopy have been developed by Bower[2] and will be briefly reviewed here.

For the Raman experiment, the intensity of scattered radiation, I_s, is given by

$$I_s = I_0 \sum \left(\sum_{i,j} l_i' l_j \alpha_{ij}\right)^2 \tag{1}$$

The summation outside the parentheses indicates that the observed intensity results from a sum over all the scattering units. The direction cosines l_i' and l_j relate the polarization vector of the incident and scattered radiation respectively to a set of axes, $O{-}X_1X_2X_3$, fixed within the sample. It is also understood that $O{-}X_3$ is the unique (drawing direction) axis of the sample. The term α_{ij} represents the ijth component of the Raman tensor of a typical structural unit. The factor I_0 is an instrumental factor depending upon the intensity of the incident light. The scattered intensity can be expressed in terms of a set of quantities that have the following form:

$$I_s = I_0 \sum \alpha_{ij}\alpha_{pq} \tag{2}$$

The individual components $\alpha_{ij}\alpha_{pq}$ are expressed as linear combinations of the principal components of the Raman polarizability tensor (α_1, α_2, and α_3) and the Euler angles between the principal axes of the tensor and the fixed axes of the sample. We define the axes of the structural units within the sample as $O{-}x_1x_2x_3$, taking $O{-}x_3$ as the c-axis. For a uniaxial specimen with no preferred orientation about the c-axis and assuming

® Abstract published in *Advance ACS Abstracts,* April 15, 1995.

0024-9297/95/2228-4007$09.00/0

that a tensor axis and the c-axis of the structural units are coincident, it is shown that[2]

$$\sum \alpha_{ij}\alpha_{pq} = 4\pi^2 N_0 \sum_l M_{l00} A_{l00}^{ijpq} \quad (3)$$

where N_0 is the number of structural units contributing to the scattering intensity, A_{l00}^{ijpq} are quadratic expressions involving the principal components of the Raman tensor that have previously been defined by Bower, and M_{l00} are the expansion coefficients of the orientation distribution function given in terms of spherical Legendre polynomials.[2] The M_{l00} are represented by

$$M_{l00} = \left(\frac{1}{4\pi^2}\right)\left(\frac{2l+1}{2}\right)^{1/2}\langle P_l(\cos\theta)\rangle \quad (4)$$

where $\langle P_l(\cos\theta)\rangle$ is the lth coefficient of the orientation distribution function for the structural units having axes $O{-}x_1x_2x_3$ defined with respect to the sample axes $O{-}X_1X_2X_3$. The angle θ is the angle between axis $O{-}x_3$ of the structural units and the unique axis of the sample. Technically the orientable components are the Raman tensors given in A_{l00}^{ijpq}. In practice, it is not necessary to study a specific vibration for which the tensor and structural unit axes are coincident. In this case it is necessary to know the relationship between the Raman tensor and the axes of the structural units in order to gain information regarding the molecular orientation of the sample.

Bower has shown that for a sample possessing uniaxial symmetry only five quantities with tensor components $\alpha_{ij}\alpha_{pq}$ are independent and nonzero.[2] These tensor components are all of the form α_{ii}^2, $\alpha_{ii}\alpha_{jj}$, and α_{ij}^2, where $i \neq j$.

The five measurable quantities are given by the following expressions:

$$I_0\sum\alpha_{22}^2 = b[\{(3a_1^2 + 3a_2^2 + 3 + 2a_1a_2 + 2a_1 + 2a_2)/15\} + P_2\{(3a_1^2 + 3a_2^2 - 6 + 2a_1a_2 - a_1 - a_2)/21\} + 3P_4\{(3a_1^2 + 3a_2^2 + 8 + 2a_1a_2 - 8a_1 - 8a_2)/280\}] \quad (5)$$

$$I_0\sum\alpha_{33}^2 = b[\{(3a_1^2 + 3a_2^2 + 3 + 2a_1a_2 + 2a_1 + 2a_2)/15\} - 2P_2\{(3a_1^2 + 3a_2^2 - 6 + 2a_1a_2 - a_1 - a_2)/21\} + P_4\{(3a_1^2 + 3a_2^2 + 8 + 2a_1a_2 - 8a_1 - 8a_2)/35\}] \quad (6)$$

$$I_0\sum\alpha_{21}^2 = b[\{(a_1^2 + a_2^2 + 1 - a_1a_2 - a_1 - a_2)/15\} + P_2\{(a_1^2 + a_2^2 - 2 - 4a_1a_2 + 2a_1 + 2a_2)/21\} + P_4\{(3a_1^2 + 3a_2^2 + 8 + 2a_1a_2 - 8a_1 - 8a_2)/280\}] \quad (7)$$

$$I_0\sum\alpha_{23}^2 = b[\{(a_1^2 + a_2^2 + 1 - a_1a_2 - a_1 - a_2)/15\} - P_2\{(a_1^2 + a_2^2 - 2 - 4a_1a_2 + 2a_1 + 2a_2)/42\} - P_4\{(3a_1^2 + 3a_2^2 + 8 + 2a_1a_2 - 8a_1 - 8a_2)/70\}] \quad (8)$$

$$I_0\sum\alpha_{22}\alpha_{33} = b[\{(a_1^2 + a_2^2 + 1 + 4a_1a_2 + 4a_1 + 4a_2)/15\} - P_2\{(a_1^2 + a_2^2 - 2 + 10a_1a^2 - 5a_1 - 5a_2)/42\} - P_4\{(3a_1^2 + 3a_2^2 + 8 + 2a_1a_2 - 8a_1 - 8a_2)/70\}] \quad (9)$$

where $b = I_0N_0\alpha_3^2$, $a_1 = \alpha_1/\alpha_3$, and $a_2 = \alpha_2/\alpha_3$. The variables P_2 and P_4 represent $\langle P_2(\cos\theta)\rangle$ and $\langle P_4(\cos\theta)\rangle$, respectively. The abbreviations P_2 and P_4 will be used to symbolize the order parameters $\langle P_2(\cos\theta)\rangle$ and $\langle P_4(\cos\theta)\rangle$ for the remainder of this paper. The first four quantities can be determined experimentally from individual polarized Raman measurements. The final quantity is calculated by combining different polarized spectra recorded with the sample at various physical orientations with reference to the laboratory axes. Using the experimentally determined intensities, eqs 5–9 are solved simultaneously, yielding values for the variables.

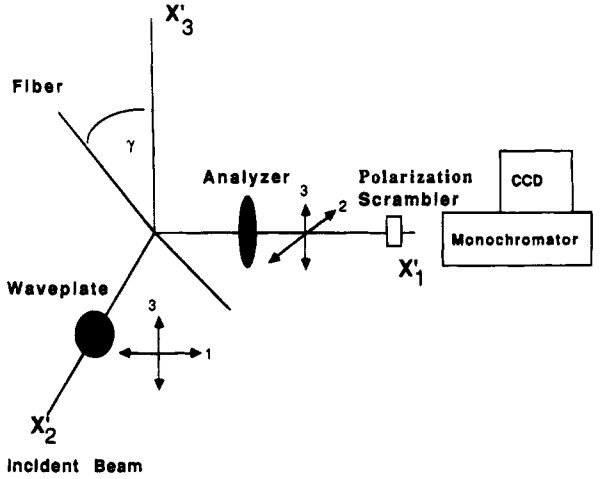

Figure 1. Arrangement of the right-angle scattering experimental geometry. The angle γ represents the angle between the drawing direction of the fiber and the laboratory axis $O{-}X_3'$.

Experimental Section

A HDPE fiber produced at the Du Pont Central Science Laboratories was used in the present study. The fiber was 10 μm thick and had a tenacity of 3.2 GPa with 3.5% elongation. The Young's modulus was 103 GPa. The degree of crystallinity estimated by differential scanning calorimetry was 80–85%.

A Spectra-Physics 2040E argon ion laser operating at 514.5 nm provided sample excitation for the Raman experiments. The power at the sample was approximately 300 mW. An adjustable half-wave plate controlled the polarization of the incident beam, and a dichroic polarizer provided polarization discrimination of the scattered radiation. A polarization filter was installed in front of the half-wave plate to ensure that only a single state of linear polarized radiation was incident upon the sample. A Spex Triplemate monochromator and Photometrics CCD 9000 detector interfaced with a Dell personal computer were used to record data. A polarization scrambler was incorporated prior to the entrance slits of the monochromator. The fiber was mounted on a 360° adjustable rotation stage. This stage was attached to an xyz translation stage to allow for the precise positioning of the sample.

X-ray diffraction patterns were obtained from a single fiber bundle using Ni-filtered Cu Kα radiation and a vacuum flat plate camera equipped with a Molecular Dynamics imaging plate. The value of $\langle P_2(\cos\theta)\rangle_{\text{X-ray}}$, which describes the orientation of the chain axis in the crystalline phase with respect to the fiber axis, was extracted from azimuthal scans through the (110) reflection after appropriate background corrections were made.

The arrangement of the Raman right-angle scattering experimental geometry used in our laboratory is shown in Figure 1. The laboratory axes $O{-}X_1'X_2'X_3'$ are also defined in the figure. For the right-angle scattering geometry, the incident beam propagates along axis $O{-}X_2'$ and the scattering direction is parallel to axis $O{-}X_1'$. The sample is aligned such that the unique axis of the sample, $O{-}X_3$, is originally parallel to $O{-}X_3'$ but may be rotated by some variable angle in the

O–$X_2'X_3'$ plane. For each angle γ, four polarized spectra $I_{ij}(\gamma)$ are recorded. The subscript i refers to the polarization vector of the scattered radiation, and j represents the polarization vector of the incident beam. The right-angle scattering polarized spectra obtained as a function of γ are given by

$$I_{21}^{RAS}(\gamma) = I_0\sum(\alpha_{21}\cos\gamma - \alpha_{31}\sin\gamma)^2 \quad (10)$$

$$I_{31}^{RAS}(\gamma) = I_0\sum(\alpha_{21}\sin\gamma + \alpha_{31}\cos\gamma)^2 \quad (11)$$

$$I_{33}^{RAS}(\gamma) = I_0\sum(\alpha_{33}\cos^2\gamma - \alpha_{23}\sin 2\gamma + \alpha_{22}\sin^2\gamma)^2 \quad (12)$$

$$I_{23}^{RAS}(\gamma) = I_0\sum\left(\frac{1}{2}\alpha_{22}\sin 2\gamma + \alpha_{23}\cos^2\gamma - \alpha_{23}\sin^2\gamma - \frac{1}{2}\alpha_{33}\sin 2\gamma\right)^2 \quad (13)$$

To acquire 180° backward scattering spectra, a small 45° mirror is inserted into the O–X_1' axis which makes the incident and scattered axes collinear. Intensity expressions analogous to eqs 10–13 can also be obtained for the backward scattering arrangement.

$$I_{22}^{BS}(\gamma) = I_0\sum(\alpha_{22}\cos^2\gamma - \alpha_{23}\sin 2\gamma + \alpha_{33}\sin^2\gamma)^2 \quad (14)$$

$$I_{33}^{BS}(\gamma) = I_0\sum(\alpha_{33}\cos^2\gamma - \alpha_{23}\sin 2\gamma + \alpha_{22}\sin^2\gamma)^2 \quad (15)$$

$$I_{23}^{BS}(\gamma) = I_{32}^{BS}(\gamma) = I_0\sum\left(\frac{1}{2}\alpha_{22}\sin 2\gamma + \alpha_{23}\cos^2\gamma - \alpha_{23}\sin^2\gamma - \frac{1}{2}\alpha_{33}\sin 2\gamma\right)^2 \quad (16)$$

To obtain the five intensities needed to solve eqs 5–9, it is usually necessary to employ the right-angle scattering configuration and record sample spectra at various angles (γ). Adjusting the position of the sample may introduce errors in the absolute intensity of the spectra recorded at different values of γ. These errors are usually accounted for by normalizing the spectra recorded at different angles.[3,6] For example, polarized spectra $I_{23}^{RAS}(0)$ and $I_{23}^{RAS}(90)$ must be identical to one another in the case of a uniaxially oriented sample. Unfortunately, recording spectra at $\gamma = 90°$ is extremely difficult in the case of a fiber. Alignment problems and polarization scrambling by the sample seem to adversely affect this measurement. Only one quantity, $I_0\Sigma\alpha_{22}^2$, needs to be recorded at $\gamma = 90°$ when the right-angle scattering geometry is employed. This quantity can also be obtained from the backward scattering geometry with $\gamma = 0°$. Superior results for the measurement $I_0\Sigma\alpha_{22}^2$ were obtained with the backward scattering geometry when compared to measurements made with the right-angle scattering configuration. For this reason we have used the backward scattering sconfiguration to measure $I_0\Sigma\alpha_{22}^2$ in this study. Since $I_0\Sigma\alpha_{33}^2$ and $I_0\Sigma\alpha_{23}^2$ can be measured from both the right-angle scattering and backward scattering geometries, absolute intensity differences between spectra obtained with the two scattering geometries are easily corrected.

Results and Discussion

The right-angle scattering polarized Raman spectra of the HDPE fiber at $\gamma = 0°$ and $\gamma = 45°$ are shown in Figures 2 and 3, respectively. The backward scattering spectra of the fiber are shown in Figure 4. The backward scattering spectra were recorded for $\gamma = 0°$ only. The right-angle and backward scattering spectra were normalized such that the absolute intensities of $I_{23}^{RAS}(0)$ and $I_{33}^{RAS}(0)$ were equivalent to $I_{23}^{BS}(0)$ and $I_{33}^{BS}(0)$ for both experimental scattering geometries. The five $I_0\Sigma\alpha_{ij}\alpha_{pq}$ spectra needed to solve eqs 5–9 are shown in Figure 5. The spectrum $I_0\Sigma\alpha_{22}\alpha_{33}$ is obtained from the following operation:

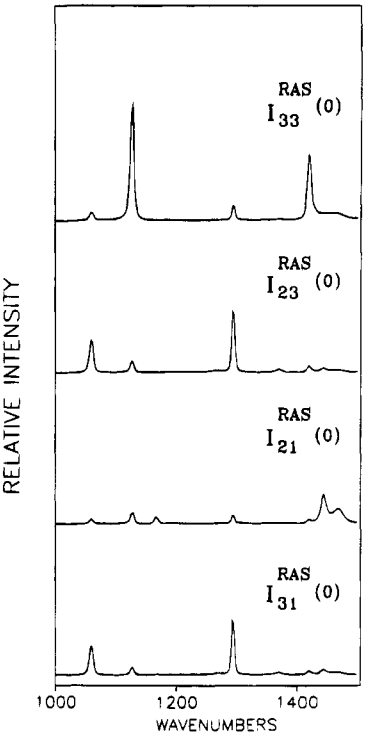

Figure 2. Four polarized $I_{ij}(\gamma)$ spectra recorded at $\gamma = 0$ obtained with the right-angle scattering experimental configuration.

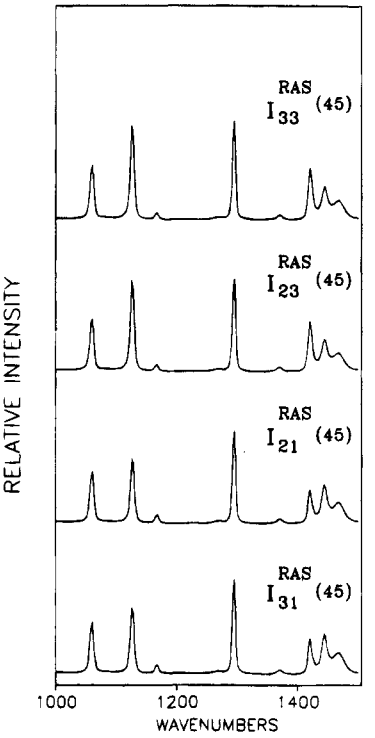

Figure 3. Four polarized $I_{ij}(\gamma)$ spectra recorded at $\gamma = 45°$ obtained with the right-angle scattering experimental configuration.

$$I_0\sum\alpha_{22}\alpha_{33} = I_{33}^{RAS}(45) - I_{23}^{RAS}(45) - I_{23}^{RAS}(0) \quad (17)$$

All the $I_{ij}(\gamma)$ were recorded with the right-angle scattering experimental configuration. This quantity may also be obtained from the following operation:

$$I_0\sum\alpha_{22}\alpha_{33} = \frac{1}{2}I_{33}^{RAS}(0) + \frac{1}{2}I_{22}^{BS}(0) - 2I_{23}^{RAS}(45) \quad (18)$$

In this case $I_{22}^{BS}(0)$ is obtained from the backward

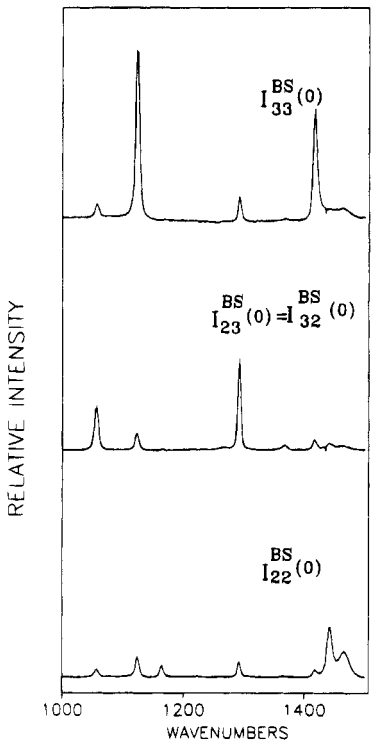

Figure 4. Polarized $I_{ij}(\gamma)$ spectra recorded at $\gamma = 0$ obtained with the backward scattering experimental configuration.

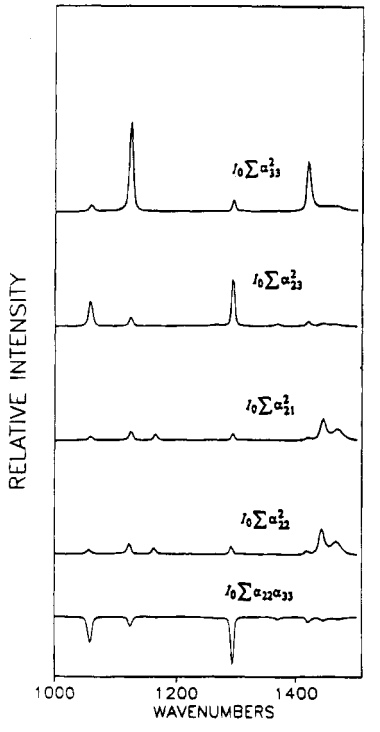

Figure 5. The five independent $I_0\Sigma\alpha_{ij}\alpha_{pq}$ spectra necessary to solve eqs 5–9.

scattering experimental geometry. Both methods must result in the desired spectrum $I_0\Sigma\alpha_{22}\alpha_{33}$. The final results for both of these operations are illustrated in Figure 6. It has been concluded that spectra measured at $\gamma = 45°$ are most susceptible to intensity errors due to sample alignment and birefringence.[2-6] Calculating $I_0\Sigma\alpha_{22}\alpha_{33}$ by the operations described in eqs 17 and 18 is a good qualitative check on the experimental data. Severe differences in sign and relative magnitude of the features in the calculated spectra are likely to be caused by birefringence effects. The good agreement between

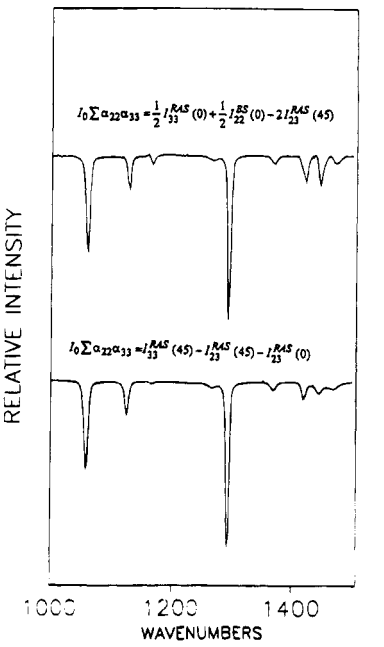

Figure 6. Calculated spectrum $I_0\Sigma\alpha_{22}\alpha_{33}$ obtained from eqs 17 (lower trace) and 18 (upper trace).

the two calculated spectra shown in Figure 6 provides some assurance that intensity errors are small. The order parameters have been computed using intensities obtained from both spectra shown in Figure 6. The order parameters calculated for the band at 1130 cm^{-1} were close in value but order parameters calculated for the 1418 cm^{-1} feature differed by approximately 15% for the two spectra shown in Figure 6. The value $\langle P_2(\cos\theta)\rangle_{Raman}$ is closer to $\langle P_2(\cos\theta)\rangle_{X\text{-}ray}$ for the feature at 1418 cm^{-1} when the intensity from $I_0\Sigma\alpha_{22}\alpha_{33}$ was obtained via eq 17. For this reason we are only reporting the order parameters calculated using intensities obtained from the lower trace in Figure 6.

The normal modes responsible for the observed features in the Raman spectrum of polyethylene have previously been assigned.[6,9-11] The feature at 1060 cm^{-1} in the Raman spectrum is assigned to C–C antisymmetric stretching modes associated with both crystalline and amorphous regions of the fiber. The absence of a band at 1080 cm^{-1}, assigned to gauche conformers in the amorphous phase, is indicative that the fiber sample is highly crystalline. Other researchers have used the feature at 1080 cm^{-1} to study the orientation of the amorphous phase.[4,6] This feature is virtually nonexistent in our spectra and no attempt is made to calculate the order parameters from this peak. The feature at 1130 cm^{-1} is assigned to symmetric C–C stretching modes of the all-trans conformation, predominantly found in the crystalline phase. The band at 1170 cm^{-1} is assigned to methylene rocking modes of the crystalline and amorphous phases. The peak at 1296 cm^{-1} is assigned to methylene twisting modes of the crystalline phase. The features from 1400 to 1460 cm^{-1} result from methylene deformation modes. The peak at 1418 cm^{-1} is characteristic of the orthorhombic crystalline phase and has previously been used to approximate the degree of crystallinity of the sample.[12] The other features in the methylene deformation region are not completely understood, although the origins of these bands have been discussed.[13,14]

For HDPE it has been established that the c-axis of the structural unit and the major axis of the Raman

Table 1. Experimentally Determined Relative Intensities for the Different $I_0\Sigma\alpha_{ij}\alpha_{pq}$

1130 cm^{-1}				
$I_0\Sigma\alpha_{33}^2$	$I_0\Sigma\alpha_{22}^2$	$I_0\Sigma\alpha_{21}^2$	$I_0\Sigma\alpha_{23}^2$	$I_0\Sigma\alpha_{22}\alpha_{33}$
1.000	0.120	0.095	0.096	−0.100
1418 cm^{-1}				
$I_0\Sigma\alpha_{33}^2$	$I_0\Sigma\alpha_{22}^2$	$I_0\Sigma\alpha_{21}^2$	$I_0\Sigma\alpha_{23}^2$	$I_0\Sigma\alpha_{22}\alpha_{33}$
1.000	0.074	0.057	0.085	−0.110

Table 2. The Four Roots to Eqs 5−9 Calculated for the Features at 1130 and 1418 cm^{-1} [a]

1130 cm^{-1}				
b	a_1	a_2	P_2	P_4
1.38	0.22	−0.51	0.76	0.49
1.38	−0.51	0.22	0.76	0.49
0.10	0.50	−4.20	−1.15	0.89
0.10	−4.20	0.50	−1.15	0.89
1418 cm^{-1}				
b	a_1	a_2	P_2	P_4
1.33	−0.43	0.14	0.82	0.53
1.33	0.14	−0.43	0.82	0.53
0.06	−4.92	0.64	−1.35	1.08
0.06	0.64	−4.92	−1.35	1.08

[a] $b = I_0N_0\alpha_3^2$, $a_1 = \alpha_1/\alpha_3$, $a_2 = \alpha_2/\alpha_3$, $P_2 = \langle P_2(\cos\theta)\rangle$, and $P_4 = \langle P_4(\cos\theta)\rangle$.

tensor coincide for vibrational modes of A_g and B_{1g} symmetry.[6] The feature observed at 1130 cm^{-1} arises from a superpositioning of A_g and B_{1g} modes, while the band at 1418 cm^{-1} is a pure A_g mode.[6] The order parameters calculated from these two features should therefore provide a quantitative description of molecular orientation for the fiber.

In order to calculate the order parameters, the relative intensities of the five $I_0\Sigma\alpha_{ij}\alpha_{pq}$ spectra must be measured for the features at 1130 and 1418 cm^{-1}. These intensities are given in Table 1. The relative intensities of the 1130 cm^{-1} band may be calculated from peak area or peak height measurements. The intensity of the 1418 cm^{-1} band is measured only by peak height since this feature is not completely separated from the other peaks in the region.

Using the relative intensities from Table 1, eqs 5−9 are solved simultaneously to yield values for all the variables, including the order parameters P_2 and P_4. Since eqs 5−9 are quadratic in a_1 and a_2, four roots to these equations exist. All four roots were calculated using the commercially available program *Mathematica*.[15] The instrumental factor b, must always be positive,[6] while only a narrow range of values of P_2 and P_4 is theoretically feasible.[16] Unreasonable solutions to these equations may therefore be discarded and the proper orientation information is preserved. The solutions to eqs 5−9 are shown for the bands at 1130 and 1418 cm^{-1} respectively in Table 2. The first two sets of solutions for the 1130 cm^{-1} feature possess values of P_2 and P_4 which fall well within the range of acceptable values in the P_2P_4 plane.[16] The final two roots do not provide physically reasonable values for the order parameters and may be ignored. For the band at 1418 cm^{-1}, the first two sets of solutions provide reasonable solutions for P_2 and P_4, while the last two roots have physically unrealistic values of the order parameters.

As expected, the order parameters for the 1130 cm^{-1} band and the 1418 cm^{-1} band are close in value. The feature at 1418 cm^{-1} is characteristic of the orthorhombic crystalline structure of HDPE,[11] and the values $P_2 = 0.82$ and $P_4 = 0.53$ provide a direct measure of the orientation within the crystalline phase. The peak at 1130 cm^{-1} is expected to contain intensity contributions from C−C symmetric stretching modes of the crystalline phase as well as C−C symmetric stretching modes of the trans conformer in the amorphous phase of the sample.[6] Since the fiber is predominantly crystalline, we expect the contributions from the amorphous region to be small. The slightly higher values of P_2 and P_4 for the 1418 cm^{-1} band are consistent with this observation. Pigeon et al. were unable to calculate order parameters from the intensities of the 1418 cm^{-1} peak for highly oriented HDPE film samples.[6] They have attributed this to unreliable intensity measurements of the 1418 cm^{-1} band due to Fermi resonance.[6] It is not clear why Fermi resonance would be present in the film samples but absent for the fiber, and it is possible that other optical mechanisms such as birefringence or polarization scrambling by the sample may have affected the intensity of the 1418 cm^{-1} band for the film measurements.

Qualitatively, our spectra are in good agreement with the spectra reported by Pigeon et al.[6] as well as our own data on several HDPE films. Pigeon et al. have calculated order parameters for the 1130 cm^{-1} band which are slightly higher than the values we are reporting for the fiber. These small differences are attributed to the degree of ordering produced as a result of different production methods of the fiber and film samples.

Quantitative confirmation of our data was provided by the X-ray diffraction analysis of the same set of fibers used in the Raman study. The value of P_2 calculated by X-ray diffraction methods was 0.84. No value for the fourth moment of the distribution function was obtained by the X-ray methods. The slight discrepancy between this value and the value of P_2 obtained from the 1418 cm^{-1} band is likely due to imperfect alignment of the fiber with respect to the laboratory axes.

Polarization scrambling by the sample is the major experimental obstacle when recording polarized Raman spectra on solid materials. Multiple reflections and refractions of the incident and scattered radiation near the surface of the sample can produce significant intensity errors in the resultant spectrum. Accounting for the difference between the refractive index of the sample and air may alleviate polarization scrambling. This is often accomplished by immersing the sample in a liquid with a similar refractive index as that of the sample.[17] Care should be taken to find a liquid with no interfering bands in the spectral region of interest. This sampling technique has been used successfully to reduce polarization scrambling by a PET fiber.[7] Incorporating carbon black or CuO powder into the material being studied has also been shown to be an effective method of reducing polarization scrambling in solid samples.[18] This technique reduces the depth of penetration of the incident laser beam and consequently attenuates some of the reflected or refracted radiation that may have been otherwise scrambled. Whether this method is applicable to the study of fibers is unclear because no simple method of uniformly applying the powder to the surface of the fiber has been devised.

As described in the experimental section inserting a polarization filter prior to the half-wave plate can also improve the quality of the measured spectra. Although emitted radiation from the laser is linearly polarized by a Brewster window, optical components such as mirrors and lenses can compromise the polarization

state of the light prior to reaching the sample. If such light is incident upon the sample, unwanted intensity errors may result. It may also be advantageous to exclusively use a backward scattering experimental geometry for spectral acquisition. Polarization scrambling may be less troublesome when a backward scattering configuration is employed since the scattered radiation arises from a small scattering volume near the surface of the sample. Without rotating the sample, three of the five quantities shown in eqs 5–9 may be measured from individual polarized Raman experiments utilizing a backward scattering configuration. In order to solve for the order parameters the values of α_1/α_3 and α_2/α_3 must be known. Provided the Raman tensor for a specific vibration is cylindrically symmetric ($\alpha_1/\alpha_3 = \alpha_2/\alpha_3$) and the value of this ratio is determined from depolarization measurements on an isotropic sample, the order parameters can be solved from measurements made with a backward scattering geometry.[5,6,8] If the Raman tensor being studied does not possess cylindrical symmetry, it may be possible to transfer known values of α_1/α_3 and α_2/α_3 from one molecule to another for similar vibrational modes. Until a standard procedure is developed that routinely accounts for intensity errors caused by polarization scrambling, it is useful to have some independent quantitative verification of the calculated data.

Conclusion

We have presented the first quantitative results regarding molecular orientation in HDPE fiber samples measured by polarized Raman spectroscopy. All five independent $I_0\Sigma\alpha_{ij}\alpha_{pq}$ spectra have been recorded for a single HDPE fiber. This is the first study to measure all five independent $I_0\Sigma\alpha_{ij}\alpha_{pq}$ spectra for a fiber sample and calculate the order parameters from these measurements. This avoids approximations regarding the symmetry of the Raman tensor when one or more of the independent $I_0\Sigma\alpha_{ij}\alpha_{pq}$ are unknown. All intensity measurements required to solve for the order parameters can be obtained exclusively by right-angle scattering or a combination of right-angle scattering and backward scattering polarized measurements.

The results indicate that the HDPE fiber we have studied is predominantly crystalline in nature and the structural units are oriented parallel to the spinning line of the fiber. Further quantitative polarized Raman studies on HDPE fiber samples produced under different processing conditions such as spinning speed will be performed in the future.

Acknowledgment. We wish to thank Yves Termonia and William C. Uy of the E. I. Du Pont CR&D Experimental Station for providing the fiber and film samples of HDPE used in the present work. Appreciation is also extended to Michel Pezolet of the University of Laval for providing HDPE films and helpful discussions.

References and Notes

(1) Ward, I. M. *Structure and Properties of Oriented Polymers*; Applied Science Publishers: London, 1975.
(2) Bower, D. I. *J. Polym. Sci., Polym. Phys. Ed.* **1972**, *10*, 2135.
(3) Purvis, J.; Bower, D. I. *J. Polym. Sci., Polym. Phys. Ed.* **1976**, *14*, 1461.
(4) Maxfield, J.; Stein, R. S.; Chen, M. C. *J. Polym. Sci., Polym. Phys. Ed.* **1978**, *16*, 37.
(5) Purvis, J.; Bower, D. I. *Polymer* **1974**, *15*, 645.
(6) Pigeon, M.; Prud'homme, R. E.; Pezolet, M. *Macromolecules* **1991**, *24*, 5687.
(7) Bower, D. I.; Ward, I. M. *Polymer* **1982**, *23*, 645.
(8) Huijts, R. A.; Peters, S. M. *Polymer* **1994**, *35*, 3119.
(9) Schachtschneider, J. H.; Snyder, R. G. *Spectrochim. Acta* **1963**, *19*, 117.
(10) Gall, M. J.; Hendra, P. J.; Peacock, C. J.; Cudby, M. E. A.; Willis, H. A. *Polymer* **1972**, *13*, 104.
(11) Hendra, P. J.; Jobic, H. P.; Marsden, E. P.; Bloor, D. *Spectrochim. Acta* **1977**, *33A*, 454.
(12) Strobl, G. R.; Hagedorn, W. *J. Polym. Sci., Polym. Phys. Ed.* **1978**, *16*, 1181.
(13) Luu, D. V.; Cambon, L.; Lapeyre, C. *J. Raman Spectrosc.* **1980**, *9*, 172.
(14) Luu, D. V.; Cambon, L.; Lafont, R. *J. Raman Spectrosc.* **1980**, *9*, 178.
(15) Wolfram, S. *Mathematica. A System for Doing Mathematics by Computer*, Wolfram Research Inc., 1991.
(16) Bower, D. I. *J. Polym. Sci., Polym. Phys. Ed.* **1981**, *19*, 93.
(17) Hendra, P. J. In *Laboratory Methods in Infrared Spectroscopy*; Miller, R. G., Ed.; Heyden Press: London, 1972.
(18) Strommen, D. P.; Nakamoto, K. *Appl. Spectrosc.* **1983**, *37*, 436.

MA946178L